Photonic Network Communications, 7:1, 97–104, 2004
© 2004 Kluwer Academic Publishers. Manufactured in The Netherlands.

Novel C-IPDM Signal Format for Suppression of Polarization Mode Dispersion

Min Rao, Lei Li, Yong Tang, Mingde Zhang
Department of Electronics Engineering, Southeast University, Nanjing, 210096 China
E-mail: lark@seu.edu.cn

Xiaohan Sun
Department of Electronics Engineering, Southeast University, Nanjing, 210096 China; Department of Electrical Engineering and Computer Science, Research Laboratory of Electronics, Massachusetts Institute of Technology, Cambridge, MA 02139 USA
E-mail: xhsun@seu.edu.cn or sunxh@mit.edu

Received June 6, 2003; Revised and Accepted July 31, 2003

Abstract. A novel chirped intra-bit polarization diversity modulation (C-IPDM) signal format is proposed. The transmission performance of C-IPDM is compared to NRZ, RZ and the common IPDM in terms of the PMD tolerance by simulation in a 40 Gb/s system. The results show that the C-IPDM format can reduce the effects of second-order PMD significantly due to the chirping characteristic and the system Q-factor is increased especially in high PMD systems.

Keywords: polarization mode dispersion (PMD), chirped intra-bit polarization diversity modulation (C-IPDM), Q-factor

1 Introduction

Polarization mode dispersion (PMD) has emerged as one of the critical hurdles for next-generation high bit rate transmission systems [1,2]. Consequently, there is a large interest in the techniques compensating or mitigating the effects of PMD, and a number of methods have been proposed. One simple method of making first-order PMD compensation is to transmit the signal at one of the input principal states of polarization (PSPs) [3,4] or receiving the signal on one of the output PSPs [3–5], which is called the principal-state-transmission (PST) method. However, in practice, a feedback signal must be connected back to the transmitter, which makes this method critically limited by control speed and operational complexity. Pan et al. [6,7] proposed the intra-bit polarization diversity modulation (IPDM) technique, the response time of which is orders of magnitude faster than the PST method. This scheme may eliminate differential group delays (DGD) as large as the bit period but it is able to compensate the PMD only to the first order. In the literature there have been several reports on the limitation of first-order PMD compensation and the necessity of higher-order PMD compensation [8,9]. Previous reports of second- or higher-order PMD compensators have used two or more sections before the receiver with each section requiring feedback control [10–13]. This scenario may produce a complex software algorithm for the control feedback signal, in which the DGD sections are correlated and changing one element may perturb the optimal solution on the other element. Many regions of local power-penalty minimum will appear for the feedback control loop [13,14], thereby making optimal system performance tracking extremely difficult.

In this paper, we propose a novel chirped-IPDM (C-IPDM) signal format. This format not only has the same advantages of IPDM, but also can reduce the effects of second-order PMD due to the chirping characteristic. To confirm the effectiveness of the novel C-IPDM signal, we have compared it with non-return to zero (NRZ), return to zero (RZ) and the common IPDM in terms of the PMD tolerance by simulation in a 40 Gb/s system.

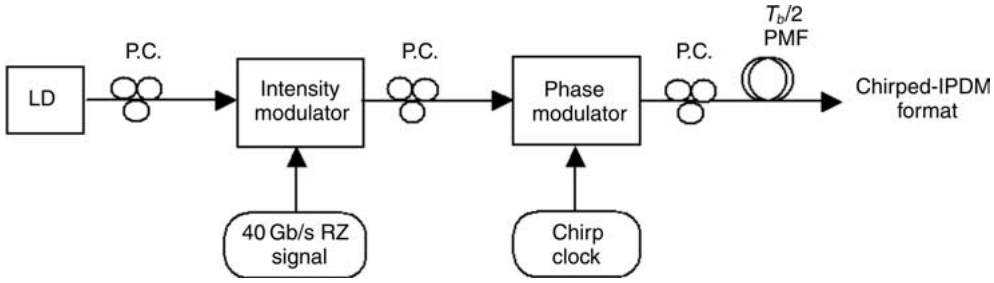

Fig. 1. Generation of proposed C-IPDM signals.

2 Proposal of Novel Chirped IPDM Signal Format

Fig. 1 shows the block diagram of the transmitter to generate the proposed signal. Using the intensity modulator, the LD output is modulated by 40 Gb/s RZ data. The phase modulator is used to generate chirp and then the chirped signal is sent through a piece of polarization maintaining fiber (PMF) with a half bit period of DGD. The chirp character of this modulation format can be set by controlling the clock frequency. In the figure, P.C. represents the polarization controller used to keep the polarization state of the signal.

3 Analysis Models

3.1 Modulation Format

The C-IPDM format contains two orthogonal polarization states per bit interval. These two orthogonal signals are staggered so that they do not overlap in the time domain and cause interference. We model this format by splitting an RZ signal, rotating the polarization in one arm and then delaying it by half a bit time prior to recombination. In our scheme, the electrical modulation signal imposes a frequency chirp on the optical carrier. Therefore, a q-bit pulse sequence of the C-IPDM format can be mathematically described as

$$E_{\mathrm{C-IPDM}}(t) = \sum_{n=1}^{q} d(t) \cdot [E_C(t - nT_b) \cos\theta + E_C(t - nT_b - T_b/2) \sin\theta], \quad (1)$$

where $d(t)$ represents the input binary data, T_b is one bit period time, θ is the angle between the input signal and the PSPs of the fiber link, and $E_C(t)$ is the output signal of the phase modulation block which can be written as

$$E_{\mathrm{C}}(t) = A \exp\left[-\frac{1}{2}\left(\frac{t}{\sigma T_b}\right)^2\right] \cdot \exp\left[\pm jC \cdot k(t)\left(\frac{t}{T_b}\right)^2\right], \quad (2)$$

where A is the peak amplitude of the RZ pulse, σ is pulse width parameter, C is the chirp factor, and $k(t)$ is the chirp inserting function. Considering different chirp inserting mode, $k(t)$ can be expressed by

- Chirp inserted in every bit: $k(t) = 1$.
- Chirp inserted in every two bits: $k(t) = \sum_{m=0}^{2m \le q-1} [\varepsilon(t - 2mT_b) - \varepsilon(t - 2mT_b - T_b)]$, where $\varepsilon(t)$ represents the step function, and $m = 0, 1, 2, \ldots$, which leads to $k(t) = 1$ in every odd bit period and $k(t) = 0$ in every even bit period.
- Chirp inserted randomly: $k(t) = \sum[\varepsilon(t - mT_{\mathrm{b}}) - \varepsilon(t - mT_b - T_b)]$, where m is randomly selected between 1 and q.

In this paper, we only discuss the case that the chirp is inserted in every bit and compare its performance with NRZ, RZ, and IPDM formats. Fig. 2 shows the input pulses and eye diagram of different modulation formats. It can be seen that the input pulse shape of C-IPDM is almost the same as that of IPDM. But due to the phase difference between them, the frequency spectrum of C-IPDM is wider than that of IPDM, which is shown in Fig. 3.

3.2 Fiber Modeling

The coupled nonlinear Schrodinger equations describing a fiber with relatively high birefringence

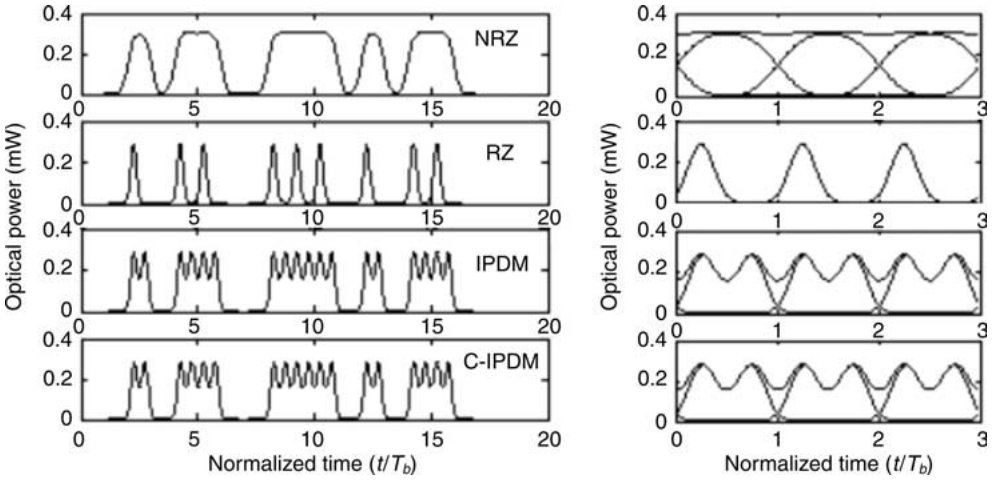

Fig. 2. The input pulses and eye diagrams of NRZ, RZ, IPDM and C-IPDM formats.

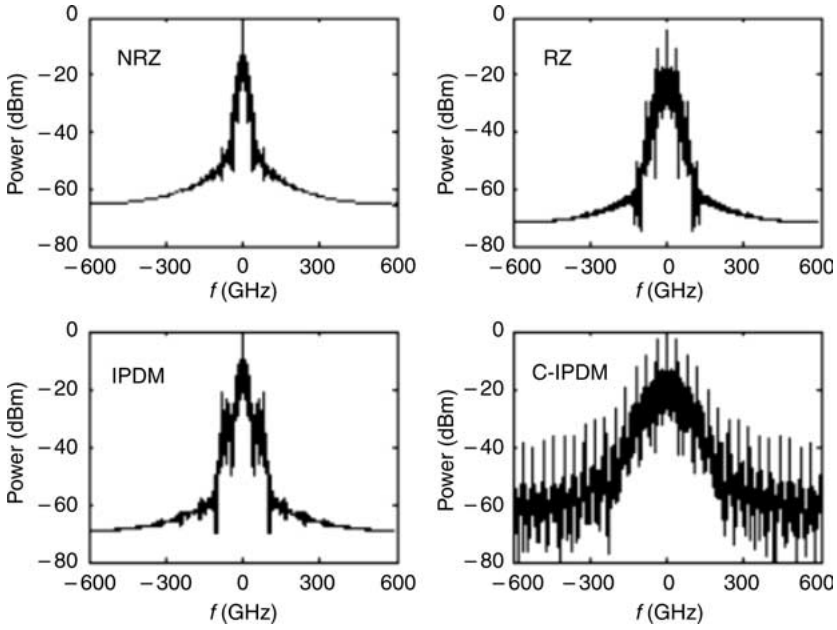

Fig. 3. The frequency spectrum of NRZ, RZ, IPDM and C-IPDM formats.

are Khosravani and Willner [15] and Matsumoto et al. [16].

$$\frac{\partial A_x}{\partial z}+\beta_x'\frac{\partial A_x}{\partial t}+\frac{i}{2}\beta''\frac{\partial^2 A_x}{\partial t^2}+\frac{\alpha}{2}A_x=i\gamma\left(|A_x|^2+\frac{2}{3}|A_y|^2\right)A_x$$
$$\frac{\partial A_y}{\partial z}+\beta_y'\frac{\partial A_y}{\partial t}+\frac{i}{2}\beta''\frac{\partial^2 A_y}{\partial t^2}+\frac{\alpha}{2}A_y=i\gamma\left(|A_y|^2+\frac{2}{3}|A_x|^2\right)A_y \tag{3}$$

where A_x, A_y are slowly varying amplitudes of the two polarization components, $\beta_x'-\beta_y'$ is the wave-vector mismatch due to linear birefringence, β'' is the group velocity dispersion parameter, α is the absorption coefficient, $\gamma=n_2\omega_0/A_{\text{eff}}c$ is the nonlinearity coefficient, with the Kerr coefficient $n_2=2.6\times\ 10^{-16}\,\text{cm}^2/\text{W}$, the effective mode area $A_{\text{eff}}=\ 52\,\mu\text{m}^2$, and c the speed of light.

Defining $b'=(\beta_x'-\beta_y')/2$, the linear part of (3) in the Fourier domain may be written in the form

$$\frac{\partial \mathbf{A}}{\partial z} + ib'\mathbf{s}\,\omega\mathbf{A} - \frac{i}{2}\beta''\omega^2\mathbf{A} = 0, \tag{4}$$

where $\mathbf{A} = (A_x, A_y)^t, \mathbf{s} = \left[\begin{smallmatrix} 1 & 0 \\ 0 & -1 \end{smallmatrix}\right]$. In the k-th interval Δz, the fiber is modeled as a concatenation of a number of N randomly oriented birefringent segments of length h, which results in a frequency-dependent, complex transfer matrix $\mathbf{T}_k(\omega) = \mathrm{e}^{i/2\beta''\omega^2\Delta z}\mathbf{M}_k(\omega)$, where $\mathbf{M}_k(\omega)$ is represented by

$$\mathbf{M}_k(\omega) = \prod_{n=1}^{N} \begin{bmatrix} \mathrm{e}^{-i(\Delta\varphi/2+\phi_{kn})} & 0 \\ 0 & \mathrm{e}^{i(\Delta\varphi/2+\phi_{kn})} \end{bmatrix} \cdot \begin{bmatrix} \cos\theta_{kn} & \sin\theta_{kn} \\ -\sin\theta_{kn} & \cos\theta_{kn} \end{bmatrix}, \tag{5}$$

where $\Delta\varphi = \sqrt{3\pi h/8}\cdot D_{PMD}\omega$ is the differential phase delay (DPD) of each segment [17], $D_{PMD}(\mathrm{ps}/\mathrm{km}^{1/2})$ is the PMD coefficient of the fiber and may be written as $D_{PMD} = 2b'\sqrt{8h/3\pi}$, θ_{kn} and ϕ_{kn} denote the random polarization and phase angle in the n-th segment of the k-th interval respectively, and are randomly generated following a uniform distribution with $\theta_{kn} \in [0, 2\pi)$ and $\phi_{kn} \in [-\pi/2, \pi/2]$.

Therefore, the solution to Equation (4) may be written as

$$\mathbf{A}(z_k + \Delta z, \omega) = \mathbf{T}_k(\omega)\mathbf{A}(z, \omega). \tag{6}$$

Dealing with the nonlinear terms in the time domain is quite straightforward, and we use the split-step Fourier method [18].

3.3 PSP Transmission Method

In the PST method, a PC is introduced before transmission, which is represented by the Jones matrix $\mathbf{B}$, and results in a total Jones matrix of the fiber

$$\mathbf{T}_{\mathrm{tot}}(\omega) = \mathbf{T}(\omega)\cdot\mathbf{B} = \prod_{k=1}^{K}\mathbf{T}_k(\omega) \cdot\mathbf{B} = \mathbf{T}_K\mathbf{T}_{K-1}\ldots\mathbf{T}_2\mathbf{T}_1 \cdot\begin{bmatrix} x & y \\ -y^* & x^* \end{bmatrix}. \tag{7}$$

In our calculation, the columns of $\mathbf{B}$ are determined by the input PSPs at the carrier frequency ω_0. Since the output PSPs can be calculated analytically as the eigenvectors $\mathbf{j}_{\pm}^{\mathrm{out}}$ to the matrix product $\mathbf{T}'\mathbf{T}^{-1}(\omega_0)$ [19], where $\mathbf{T}'$ is the derivative of the Jones matrix $\mathbf{T}(\omega)$ with respect to the angular frequency ω and $\mathbf{T}^{-1}$ is the inverse of $\mathbf{T}(\omega)$. The input eigenvectors are then obtained by $\mathbf{j}_{\pm}^{\mathrm{in}} = \mathbf{T}^{-1}(\omega_0)\mathbf{j}_{\pm}^{\mathrm{out}}$, from which the input polarization state should be chosen for PSP transmission.

4 Results and Discussion

4.1 Output Pulses and Eye Diagrams

Fig. 4 shows the shape of output pulses and eye diagrams for different modulation formats in 40 Gb/s systems at 10 ps and 17 ps total accumulated PMD. All simulations reported here are run without fiber losses, chromatic dispersion, and nonlinear effects. When the total PMD of the system is not very large (10 ps) as in Fig. 4(a), the eyes of NRZ, RZ and IPDM formats are still open, but the pulses are broadened and adjacent pulses merge together. For the C-IPDM format, pulse compression can be observed, and the received data pattern shows two or more distinct peaks in each time slot. If we only choose the highest peak for sampling and detection, the Q-factor can be improved compared to chirp-free IPDM. As the total PMD increased to 17 ps as in Fig. 4(b), the eye diagrams of NRZ and RZ are almost closed. For IPDM pulses, the eye is distorted but it is open wider than in the NRZ and RZ cases. For the C-IPDM format, compression helps the pulses cancel out part of the broadening caused by PMD and a widest open eye is observed.

4.2 Second-Order PMD Tolerance

To demonstrate the advantage of C-IPDM for suppressing the second-order PMD effects, we use the simplified model described in Rao et al. [20]. Here the depolarization is not taken into account, and it is assumed that there is no power coupling between the two modes of a birefringent fiber. This is a real case only for fibers shorter than the coupling length between the principal axes, or whenever the principal axes can be assumed constant over the signal spectrum. In these cases, the first-order PMD is compensated completely and the second-order PMD becomes the main limiting factor to the transmission performance. Fig. 5 shows the output pulses and the Q-factor penalty of the IPDM and C-IPDM formats. In the C-IPDM case, pulse compression can be observed and the performance is better than IPDM apparently. As we know, the second-order PMD represents the DGD linear frequency dependence and the signal chirp leads to the different frequency between the edges of the pulse. Therefore, the pulse

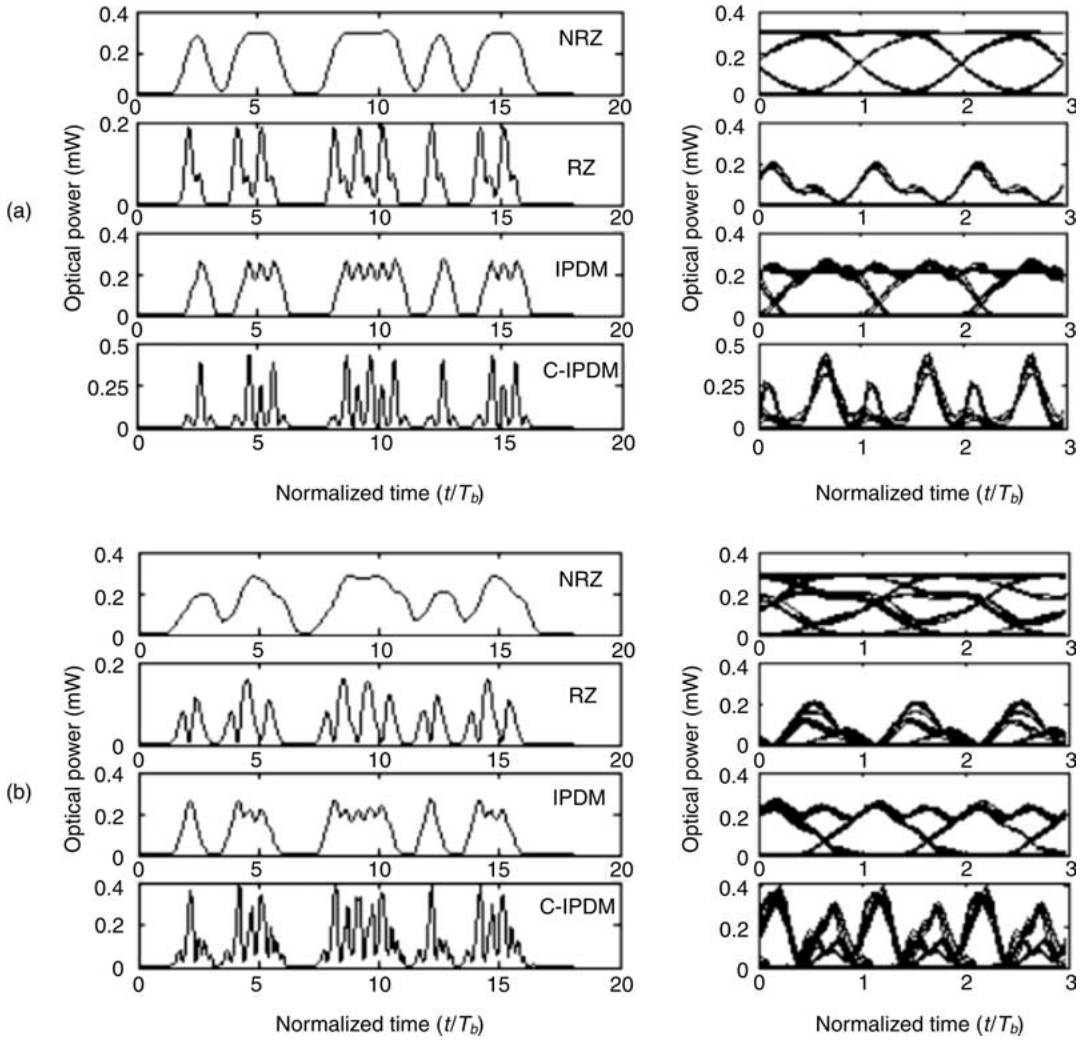

Fig. 4. The output pulses and eye diagrams for different modulation formats in 40 Gb/s systems. Average accumulated DGD is (a) 10 ps; (b) 17 ps.

will be compressed if the transmission speed of leading edge is slower than that of the trailing edge. The results can be obtained on the condition that the chirp sign is set opposite to that of the chirp induced by second-order PMD.

4.3 The Effect of Chirp

Fig. 6 shows the output pulses and eye diagram for different chirp parameter $(C = 0, 1, 2, 3)$ with 8 ps average accumulated PMD. The chirp character has significant impact on the C-IPDM format transmission performance. When $C = 2$ the format has the largest eye opening and apparent pulse compression. But this also increases the difficulty of choosing the sampling time for the receiver. On the other hand, the signal with larger chirp has wider frequency spectrum. Therefore, the chirp parameter should be selected appropriately.

4.4 Q Distribution

Fig. 7 shows the Q-factor probability density function for different modulation formats in a 40 Gb/s system with 20 ps of average DGD. For all the cases, the Q-factor is assumed to be $\sim$ 17.8 dB with no PMD in the link. The Q-factor can vary over a wide range depending on the birefringence of different segments of the transmission fiber. The Q-factor of the IPDM format is larger than the NRZ and RZ formats due to

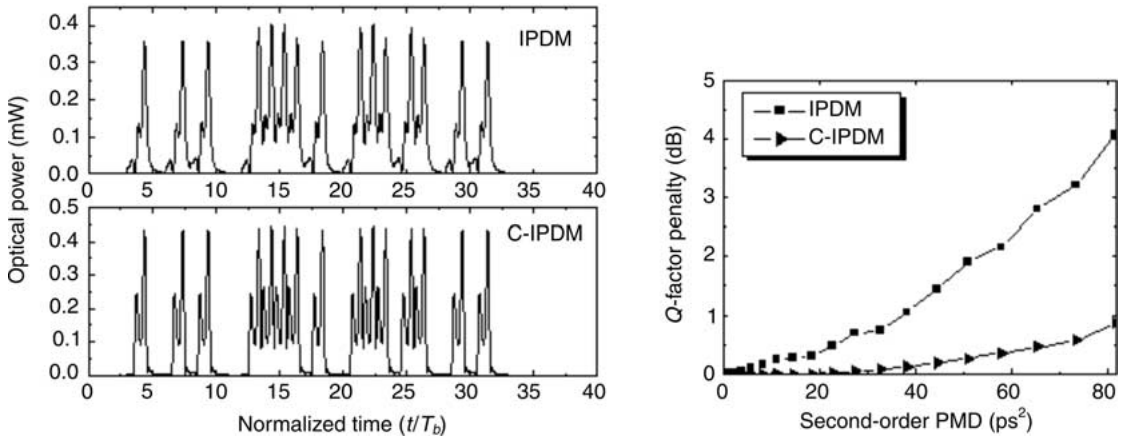

Fig. 5. The effects of second-order PMD on the transmission performance of IPDM and C-IPDM formats. (a) The output pulses when the second-order PMD is 80 ps^2; (b) The Q-factor penalty of IPDM and C-IPDM as function of second-order PMD.

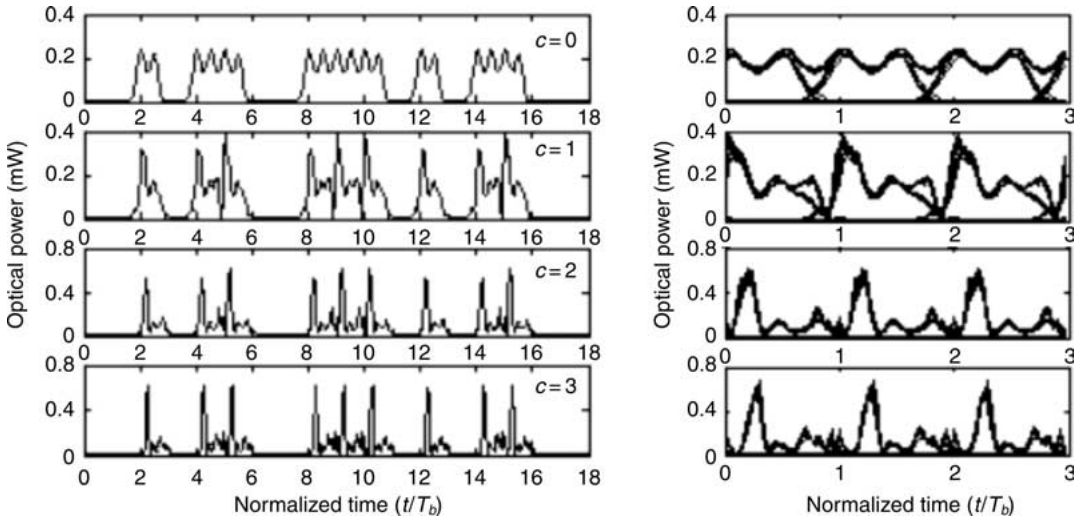

Fig. 6. The output pulses and eye diagram for different chirp parameter $(C = 0, 1, 2, 3)$ with 8 ps average accumulated DGD.

the first-order PMD compensation. The effect of the second-order PMD and the pre-chirp is to broaden the Q-factor distribution and move to higher values. Therefore, the C-IPDM format has a larger average Q-factor than the IPDM format.

4.5 Q penalty

Fig. 8 shows the Q-factor penalty vs. distance for 40 Gb/s systems with different modulation formats. The PMD induced Q-factor penalty is defined as $p_Q = -20\ \log(Q/Q_0)$, and Q_0 is the Q-factor without PMD and is assumed to be ~ 17.8 dB for all formats. Here D_{PMD} is assumed to be 0.3 ps/km$^{1/2}$ and the Q-factor is obtained by averaging over 100 orientations of PMD. As a result of PMD pulse broadening and intersymbol interference, the Q-factor penalty grows fast in the NRZ and RZ cases. But RZ pulses perform better than the NRZ because they have shorter duty cycles with a wider margin that allows them to retain their pulse power during a bit time. For the C-IPDM format, the pulses compression caused by chirping and second-order PMD leads to better performance than IPDM.

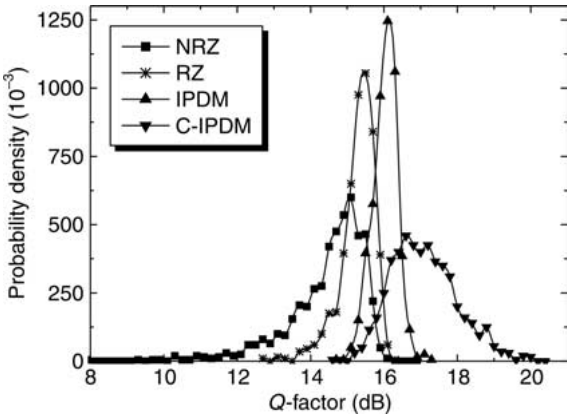

Fig. 7. The Q-factor probability density function for different modulation formats in a 40 Gb/s system with 20 ps of average DGD.

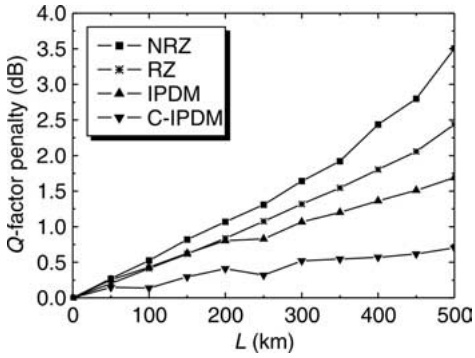

Fig. 8. The Q-factor penalty versus distance for 40 Gb/s systems with different modulation formats.

5 Conclusion

A novel chirped-IPDM signal format is proposed. The transmission performance of C-IPDM is compared to NRZ, RZ and the common IPDM in terms of the PMD tolerance by simulation in 40 Gb/s system. The results show that the C-IPDM format can reduce the effects of second-order PMD significantly due to the chirping characteristic and the system Q-factor is increased especially in high PMD systems.

Acknowledgment

This work has been supported by the National Natural Science Foundation of China (Grant No. 60272048).

References

[1] C. Francia, F. Bruyère, D. Penninckx, M. Chbat, PMD second-order effects on pulse propagation in single-mode optical fibers, IEEE Photon. Technol. Lett, vol. 10, no. 12, (December 1998), pp. 1739–1741.

[2] F. Bruyère, Impact of first-and second-order PMD in optical digital transmission systems, Opt. Fiber Technol, vol. 2, no. 3, (March 1996), pp. 269–280.

[3] J. Cameron, L. Chen, X. Bao, Anomalous pulse-width narrowing with first-order compensation of polarization mode dispersion, Opt. Lett, vol. 25, no. 6, (June 2000), pp. 884–886.

[4] Z. Haas, C. D. Poole, M. Santoro, J. H. Winters, Fiber-optic polarization dependent distortion compensation, U.S. Patent 5, (May 1994), pp. 311–346.

[5] H. Sunnerud, M. Karlsson, P. Anderkson, Analytical theory for PMD-compensation, IEEE Photon. Technol. Lett, vol. 12, no.1, (January 2000), pp. 50–52.

[6] Z. Pan, Y. Wang, C. Yu, et al., Intra-bit polarization diversity modulation for PMD mitigation, Proc. of ECOC'01 (Amsterdam, The Netherlands, 2001), vol. 3, pp. 450–451.

[7] Z. Pan, Q. Yu, A. E. Willner, Fast XPM-induced polarization-state fluctuations in WDM systems and their mitigation, OFC'2002 (Anaheim, CA, USA, March 2002), Paper ThA7, pp. 379–381.

[8] H. Bulow, System outage probability due to first-and second-order PMD, IEEE Photon. Technol. Lett, vol. 10, no. 5, (May 1998), pp. 696–698.

[9] H. Büllow, Optical Fiber Communication Conference (OFC), 1999 OSA Technical Digest Series (Optical Society of America, Washington, D.C., 1999), p. 74.

[10] Q. Yu, L. S. Yan, Y. Xie, M. Hauer, A. E. Willner, Higher order polarization mode dispersion compensation using a fixed time delay followed by a variable time delay, IEEE Photon. Technol. Lett, vol. 13, no. 8, (August 2001), pp. 863–865.

[11] M. Shtaif, A. Mecozzi, M. Tur, J. A. Nagel, A compensator for the effects of high-order polarization mode dispersion in optical fibers, IEEE Photon. Technol. Lett, vol. 12, no. 4, (April 2000), pp. 434–435.

[12] M. C. Parker, S. D. Walker, Multiple-order PMD compensation using a single actively chirped AWG, Proc. European Conf. Optical Communication (ECOC'01), (Amsterdam, The Netherlands, 2001), PaperWe.P.23.

[13] R. Noé, D. Sandel, M. Yoshida-Dierolf, S. Hinz, V. Mirvoda, A. Schöpflin, C. Glingerner, E. Gottwald, C. Scheerer, G. Fischer, T. Weyrauch, W. Haase, Polarization mode dispersion compensation at 10, 20, and 40 Gb/s with various optical equalizers, IEEE Journal of Lightwave Technology, vol. 17, no. 9, (September 1999), pp. 1602–1616.

[14] D. Penninckx, S. Lanne, Ultimate limits of optical polarizationmode-dispersion compensators, Proc. European Conf. Optical Communication (ECOC'00), (Munich, Germany, 2000), Paper P.3.8

[15] R. Khosravani, A. E. Willner, System performance evaluation in terrestrial systems with high polarization mode dispersion and the effect of chirping, IEEE Photon. Technol. Lett, vol. 13, no. 4, (April 2001), pp. 296–298.

[16] M. Matsumoto, Y. Akagi, A. Hasegawa, Propagation of

solitons in fibers with randomly varying birefringence, effects of soliton transmission control, IEEE Journal of Lightwave Technology, vol. 15, no. 4, (April 1997), pp. 584–589.
[17] A. O. Forno, A. Paradisi, R. Passy, et al., Expermental and theoretical modeling of polarization mode dispersion in single mode fibers, IEEE Photon. Technol. Lett, vol. 12, no. 3, (March 2000), pp. 296–298.
[18] G. P. Agrawal, Nonlinear Fiber Optics (New York, Academic, 1995).
[19] B. L. Heffner, Automated measurement of polarization mode dispersion using Jones Matrix Eigenanalysis, IEEE Photon.Technol Lett, vol. 9, no. 9, (September 1992), pp. 1066–1069.
[20] M. Rao, X. H. Sun, M. D. Zhang, Impact of polarization mode dispersion on high-speed optical codes, Engineering Science, vol. 4, no. 11, (November 2002), pp. 67–70.

Min Rao received her B.E. degree in 1999 from the Department of Electronic Engineering Southeast University, where she is currently working toward her Ph.D. degree. Her research interests are high-speed optical communication systems, wavelength division multiplexed optical networks, polarization mode dispersion in optical fibers, and related topics.

Lei Li received his B.S. and M.S. degrees from Department of Electronic Engineering of Southeast University in 2000 and 2002, respectively. Currently, he is working toward the Ph.D. degree at the same university. His research interests focus on high-speed optical communication systems, WDM optical networks, and related topics.

Yong Tang received his B.E. and M.S. degrees in Biomedical Engineering from Southeast University, Nanjing, China, in 1993 and 1996, respectively. From 1996 to 1999, he worked for the Nanjing Science & Technology Bureau, with responsible for the software development of industrial networks. After then, he entered Southeast University and received a Ph.D. degree in Electronic Engineering in 2003. His doctoral research focused on the node management technology in WDM optical networks, in particular the dynamic resource allocation, the transmission performance analysis and on-line signal quality monitoring. He is currently a network system engineer for Jiangsu Telecom Transmission Bureau, Nanjing, China.

Mingde Zhang, a professor of electronics engineering, Southeast University, Nanjing, China. From 1985 to 1986 he was the visiting scholar at Research Center of Laser, South California University, USA. His current research interests are optical fiber communications and system, high-speed broadband optical fiber networks, optical fiber amplifies, nonlinear fiber optics, optical waveguide devices and so on.

Xiaohan Sun, a professor of Electronics Engineering, Southeast University, Nanjing China. She has been the visiting professor at Research Lab of Electronics, MIT, USA since 2002. Her current research interests are high-speed optical communication systems including (a) optical pulse propagation in WDM systems influenced by nonlinear effects, PMD, crosstalk and so on, (b) on-line supervisory technology and dispersion management of the networks, and (c) architecture and management on WDM networks; PLCs and photonic waveguide devices including (a) simulation methods of the devices used in optical networks, (b) characteristics analysis of the devices, (c) design and measurement for GaAs/InP based PLCs, and (d) mode converters for efficient coupling of these devices with optical fibers; Optical fiber sensor technology and optical imaging.